JOURNAL OF MATERIALS PROCESSING TECHNOLOGY 203 (2008) 46–57

journal homepage: www.elsevier.com/locate/jmatprotec

Characterization of the influences of FSW tool geometry on welding forces and weld tensile strength using an instrumented tool

D.G. Hattingh[a,*], *C. Blignault*[a,c], *T.I. van Niekerk*[a], *M.N. James*[a,b]

[a] *Faculty of Engineering, Nelson Mandela Metropolitan University, Port Elizabeth 6001, South Africa*
[b] *School of Engineering, University of Plymouth, Drake Circus, Plymouth, Devon PL4 8AA, UK*
[c] *TWI, Friction and Forge Processes Section, Granta Park, Great Abington, Cambridge CB21 6AL, UK*

ARTICLE INFO

Article history:
Received 29 August 2007
Received in revised form
2 October 2007
Accepted 8 October 2007

Keywords:
Friction stir welding
Force footprint
Instrumented tool
Process optimisation
Force monitoring
Tool torque
Tool design

ABSTRACT

FSW process automation is essential to making consistent and reliable friction stir welds and this requires an understanding of how tool design can influence process parameters, which in turn can provide high joint strength and performance. Tool optimisation hinges on a better understanding of the effect of tool parameters on forces during welding, on the tool torque and tool temperature. Important parameters include flute design (e.g. number, depth, and taper angle), the tool pin diameter and taper, and the pitch of any thread form on the pin. These influences were investigated in this study using a systematic tool profile matrix which considered the influence of four variations of each of these six geometric factors. Forces on the tool, applied torque and temperature were monitored and recorded during welding of 6 mm thick 5083-H321 aluminium alloy. The lateral reaction forces on each tool and the relative angle of orientation of the peak resultant force are described via a bi-lobed polar plot called the "force footprint" (FF). This provides visual information on the interaction between tool profile and the plastic stir zone, which cannot be obtained purely from force magnitude information. Key characteristics of the tool–weld interaction can be extracted, analysed and summarized to provide guidance on optimum tool selection for a given set of weld conditions.

© 2007 Elsevier B.V. All rights reserved.

1. Introduction

Friction stir welding (FSW) was developed at TWI in 1991 and is successfully being applied to an increasing number of joining applications worldwide. FSW uses a non-consumable tool to generate frictional heat at the point of welding, inducing complex plastic deformation of the workpiece along the joint line. Generally the plates to be joined are placed on a rigid backing plate and clamped to prevent the faying joint faces from separating. A shouldered cylindrical tool, with a specially shaped pin (probe), is then rotated and slowly plunged between the faying surfaces. This causes frictional heating of the plates, which in turn lowers their mechanical strength. After a certain dwell time weld traverse starts whilst a relatively high axial load (z-force) is maintained (by a forwards rake angle) on the tool shoulder behind the pin to support weld forging. After welding the tool extracts from the plate to leave a characteristic keyhole.

During welding the tool profile is the primary cause of the mixing and recombining of the plasticized material that

* *Corresponding author at*: Summerstrand Campus (North), Nelson Mandela Metropolitan University, PO Box 77000, Port Elizabeth, 6031, South Africa. Tel.: +27 41 504 3608; fax: +27 41 504 9123.
E-mail address: Danie.Hattingh@nmmu.ac.za (D.G. Hattingh).
0924-0136/$ – see front matter © 2007 Elsevier B.V. All rights reserved.
doi:10.1016/j.jmatprotec.2007.10.028

forms the so-called weld 'third-body' region. This region is also termed the thermo-mechanically affected zone (TMAZ). The form of the tool geometry and selection of process parameter settings are therefore essential starting points for development of optimisation strategies. Tool design improvement rests on measuring the forces exerted by the third-body region on the tool during welding. Process parameters or tool geometries that minimize these forces, whilst retaining mechanical properties, will increase process efficiency and reduce the heat input required during welding. Process forces and the plastic flow around the tool are increasingly recognised as crucial to improved understanding and control of the FSW process (Arbegast, 2005; Schmidt and Hattel, 2005).

Measurement of these lateral bending forces on the tool can be automated and their subsequent analysis aided through a graphical representation of the bending force vector experienced by the tool during a single revolution. The authors have termed this diagram the force footprint (FF) (Hattingh et al., 2004). This force footprint can provide information on two orthogonal forces on the tool during rotation, on their angles relative to the weld line, and on the resultant bending force. It therefore provides a very direct way of assessing the effects of modifications to tool geometry, and of changes to parameters such as tool feed and speed during real-time applications. The monitoring system also measures tool torque, tool temperature and vertical force on the tool shoulder during welding. Generating force footprint diagrams requires integration of reliable and accurate sensor outputs from an instrumented FSW machine into a computerized control program. Such an instrumented FSW set-up, including a multi-axial transducer, has been developed, calibrated and extensively tested at the Manufacturing Technology Research Centre (MTRC) of the Nelson Mandela Metropolitan University in Port Elizabeth, South Africa (Blignault, 2003, 2006; Lombard, 2007).

This paper concentrates on relating changes in these parameters to specific tool geometry changes in order to gain insight into conditions in the plasticised third-body region during welding. In principle, once these relationships are understood, tool speed, feed and profile can be intelligently changed in response to changing weld joint requirements. It should be noted that tool performance is assessed in this paper in terms of the required weld output property of mechanical strength, and in terms of the weld process parameters that will reflect plastic deformation and flow in the alloy. Microstructure per se is not a controlling parameter in this 5083-H321 alloy as a variety of weld process conditions give rise to very similar equiaxed grain sizes in the nugget and to similar grain elongation in the TMAZ region (Lombard, 2007). Previous work by the authors on this alloy has shown that tensile properties and fatigue performance are governed by more subtle effects of plastic flow processes, in particular the development of planar pseudo-bonds between entrained streams of plastic material (James et al., 2005; Lombard et al., 2008). Process conditions that optimise tensile strength therefore also lead to good plastic flow around the tool and to optimised defect population and microstructure.

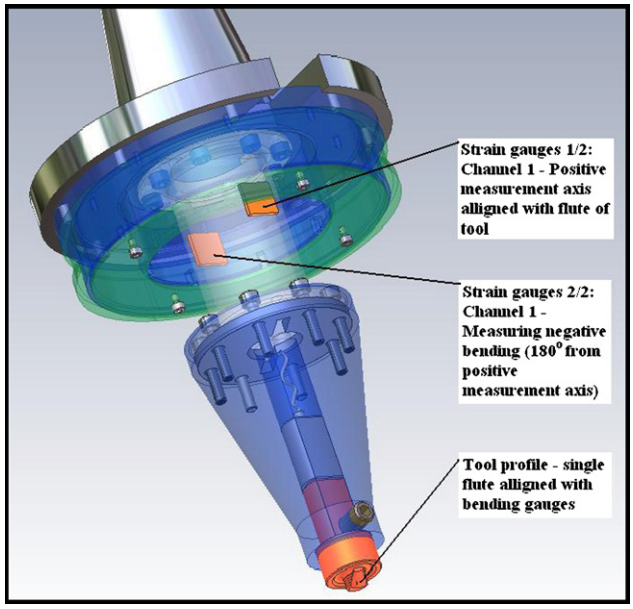

Fig. 1 – Illustration of the definition of a zero rotational angle. The position of one the strain gauges on the tool holder assembly coincides with a tool flute.

2. Overview of the multi-axial transducer and the force footprint (FF)

This section outlines the main features of the monitoring system and the development of the FF. Further information is contained in Hattingh et al. (2004), Blignault (2003, 2006), Lombard (2007) and Blignault et al. (2008). The bending forces exerted on the tool during welding can be plotted against the angular position of the tool to provide a polar FF diagram (see Fig. 3). This polar plot identifies the peak force during any revolution of the tool and its orientation relative to the direction of welding. The data are captured at specific rotational intervals using strain gauges in a full bridge configuration which rotates with the tool holder. The design of the tool holder ensures that FSW tools are kept in a constant reference position during tool changes. This reference position is taken as the case where one of the bending axis strain gauges mounted on the tool is aligned with a flute on the tool pin as illustrated in Fig. 1. This is then identified as the 0° position in all subsequent analysis.

A spindle encoder (mounted on top of the rotating spindle) counts from a fixed reference position and completes one revolution when 7200 pulses have been made. When a bending moment is introduced on the tool during welding the magnitude and direction of the resultant maximum and minimum forces can be detected during each tool revolution. This data can be resolved using vector arithmetic to give x-axis and y-axis forces at any point during rotation. Measurement of these signals during one full revolution produces a sinusoidal waveform. The polar plot of such force data gives a characteristic force footprint diagram which is influenced by the weld process conditions (e.g. tool speed and feed, tool geometry, and alloy). Combining the data from the two orthogonal forces gives a resultant load force footprint, the area of which can be related to energy input into the weld. However, the maximum

bending load on the tool and its orientation can be obtained from the larger single force polar plot. The angle of rotation of this peak force is believed to reflect plastic flow conditions around the tool. Thus the force footprint should offer useful insights into metallurgical conditions during welding and can assist in identifying optimum process conditions in terms of mechanical properties of welds, and their fatigue and fracture performance.

Applied torque and compressive loading on the tool (z-force) during welding are also recorded by strain gauges situated on the tool holder. An insulated thermocouple, which has a 0.5 mm diameter probe and a typical response time of 0.15 s, is embedded in the tool and provides information on tool temperature. Data from all these channels are recorded simultaneously at 1 kHz during welding. The data is transmitted from the rotating tool holder by radio telemetry while an inductive rotor and stator coil unit are responsible for power transmission to the strain gauges.

3. Analysing the force footprint

Amongst other uses, the FF can be employed as a tool to analyse FSW process behaviour as a function of tool geometry. This should enable a reduction in the current empiricism associated with choosing FSW process conditions and lead to the design of more efficient tools. The current work aims to investigate the role of tool parameters on forces during welding, on the value of the required torque and on tool temperatures. Important parameters include the flute geometry (e.g. number, depth, and taper angle), the tool pin diameter and taper, and the pitch of any thread form on the pin. To examine this problem a systematic tool profile matrix was used which considered the influence of four variations of each of these six geometric factors. These tool geometries are shown in Fig. 2 and as part of the FF plot in Figs. 3–8 and their performance was evaluated under a constant set of process input conditions as given in Table 1. The FSW machine did not control z-force and therefore the downwards z-axis force was treated as a dependant process response variable.

Table 2 summarizes the permutations of the various tool geometry parameters chosen for this investigation. These tool modifications were intended to give a comparative study of the trends in process parameters and tensile strength as a function of progressive changes in each parameter. Fig. 2 shows machining details of the various tools. The remainder of the paper will summarise and discuss the data recorded during welding as a function of these tool parameters. The recorded data for each tool type in the experimental matrix represent the average of four separate tests. Table 3 summarises the ranges of weld process parameters found for each tool series. Note that a minimum or maximum value of one parameter does not generally occur in conjunction with that of another parameter for any given tool. The data are all compared at a specific point during the welding process, namely at a weld length of 245 mm which is some 33% of the total weld run and is in a region of the process where nominally steady-state conditions occur. Tools were machined with a constant thread pitch of 1 mm on the pin except for the case of H-series tools where pitch was the variable to be explored. The standard pin diameter was 10 mm.

It is also important to note that many of these tools produced defective welds with a relatively high percentage of voids in the cross-section; part of the intention of the experimental matrix was to explore the tool parameters that led to defect-free welds and to highly defective welds. Defect information is captured implicitly in the recorded values of weld tensile strength, which can be compared with the parent plate tensile strength of 348 MPa. Tools A2, A3, D4, F1, F2, F4, P4, T3 and T4 produced welds which were free of voids at a macroscopic level. Tools A3, D3, F1, P4, H2 and T4 produced the highest strength welds in their series. There is hence a corre-

Table 1 – Process input conditions used to evaluate the performance of all tools

Spindle speed during tool plunge	600 rpm
Weld length	750 mm
Plunge feed rate	10 mm/min
Clearance between pin and backing bar	~0.1 mm
Dwell time	8 s
Weld feed rate	150 mm/min
Weld spindle speed	500 rpm
Tool tilt angle	2.5°
Plate thickness	6 mm
Parent material	AA5083–H321
Pin length	5.7 mm

All tools used the same conical shoulder design.

Table 2 – Relative changes in the chosen tool parameters

Tool matrix				Tool parameter change
A1	A2	A3	A4	Increase in number of flutes (1 → 4)
D1	D2	D3	D4	Increase in flute depth (1 → 4)
F1	F2	F3	F4	Increase in flute angle (1 → 4)
T1	T2	T3	T4	Increase in pin taper angle (1 → 4)
P1	P2	P3	P4	Decrease in pin diameter (1 → 4)
H1	H2	H3	H4	Increase in thread pitch (1 → 4)

Table 3 – Summary of weld process parameter ranges for each tool series

Tool series	Temperature range (°C)	Torque range (Nm)	Maximum force range (N)	Tensile strength range (MPa)
A	506–576	58.1–64.3	2713–5471	184–290
D	551–601	55.8–65.0	3043–4605	141–256
F	566–583	42.2–63.2	3369–3829	160–337
T	497–552	46.0–53.8	2881–3546	209–331
P	526–572	45.7–67.2	3507–5100	10–207
H	553–575	46.7–59.8	3828–5019	110–174

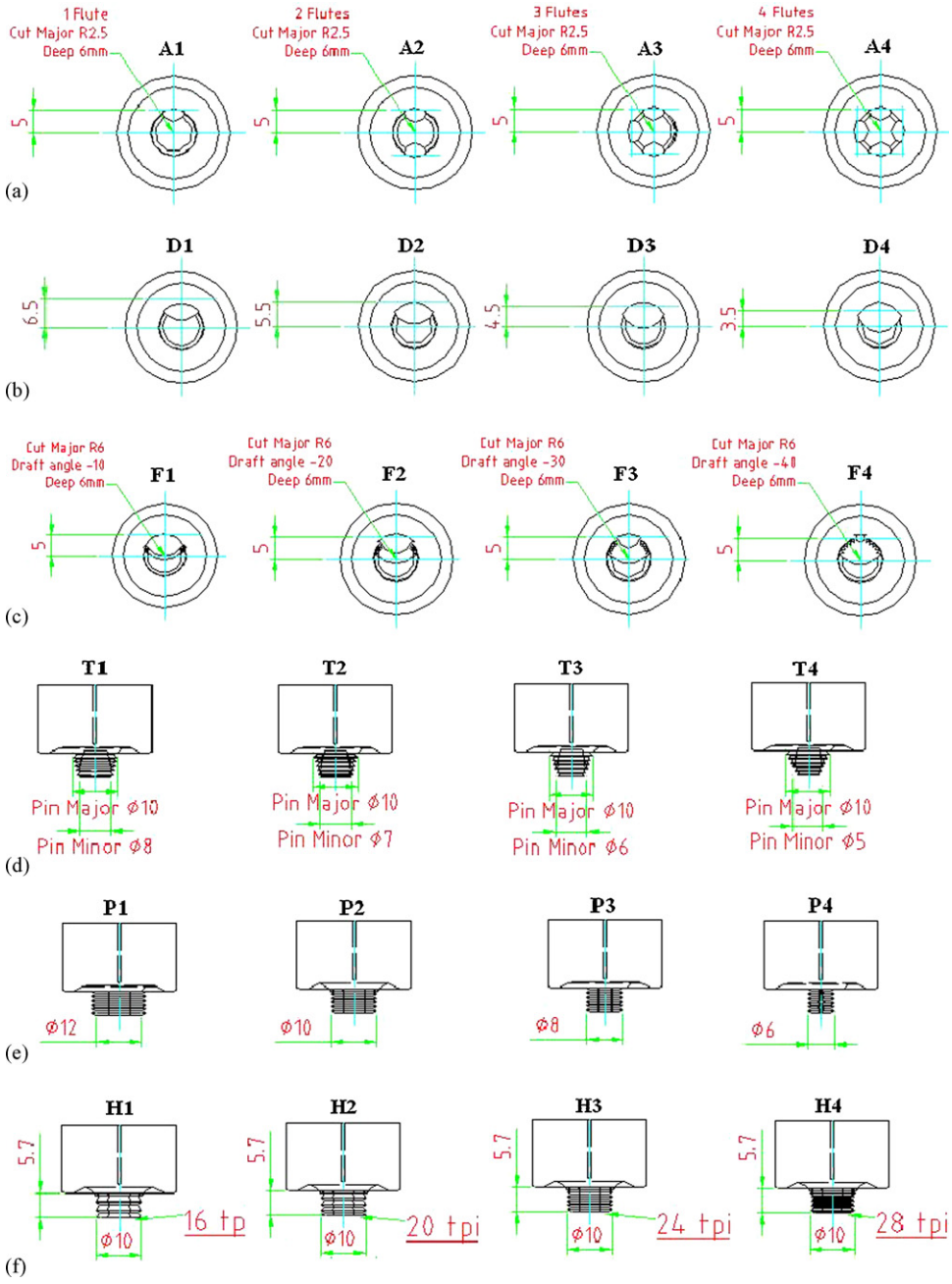

Fig. 2 – (a) Pin flute details on A-series tools; (b) pin flute depth details on D-series tools; (c) pin flute angle details on F-series tools; (d) pin taper details on T-series tools; (e) pin diameter details on P-series tools; (f) pin thread details on H-series tools.

lation between the presence of defects (voids) and the highest strength welds for tools series A, F and P. Series F and A tools produced the highest and third highest strength welds found with this experimental matrix, while tool series D produced the second highest strength weld. Tool series P produced generally highly defective welds. The interpretation of this data is that for tool series producing the very highest and lowest strength welds, defects like voids control the tensile properties. However, for the case of high performance welds made with tool series D, H and T other plastic flow effects (pseudo-bond defects (James et al., 2005)) are important in producing high strength friction stir welds.

4. Number of flutes (A-series tools)

This tool series was characterized by a variation in number of flutes from one flute on tool A1 to four flutes on tool A4. The geometries are illustrated in Figs. 2a and 3a, which also presents the force footprint data for the four tools and gives summary tables of the measured parameters. Note that B is the lateral (bending) force on the tool during welding and that the tables give maximum and minimum measured values of this force. Also note that the tool is moving horizontally from left to right in these figures. To aid interpretation Fig. 3b

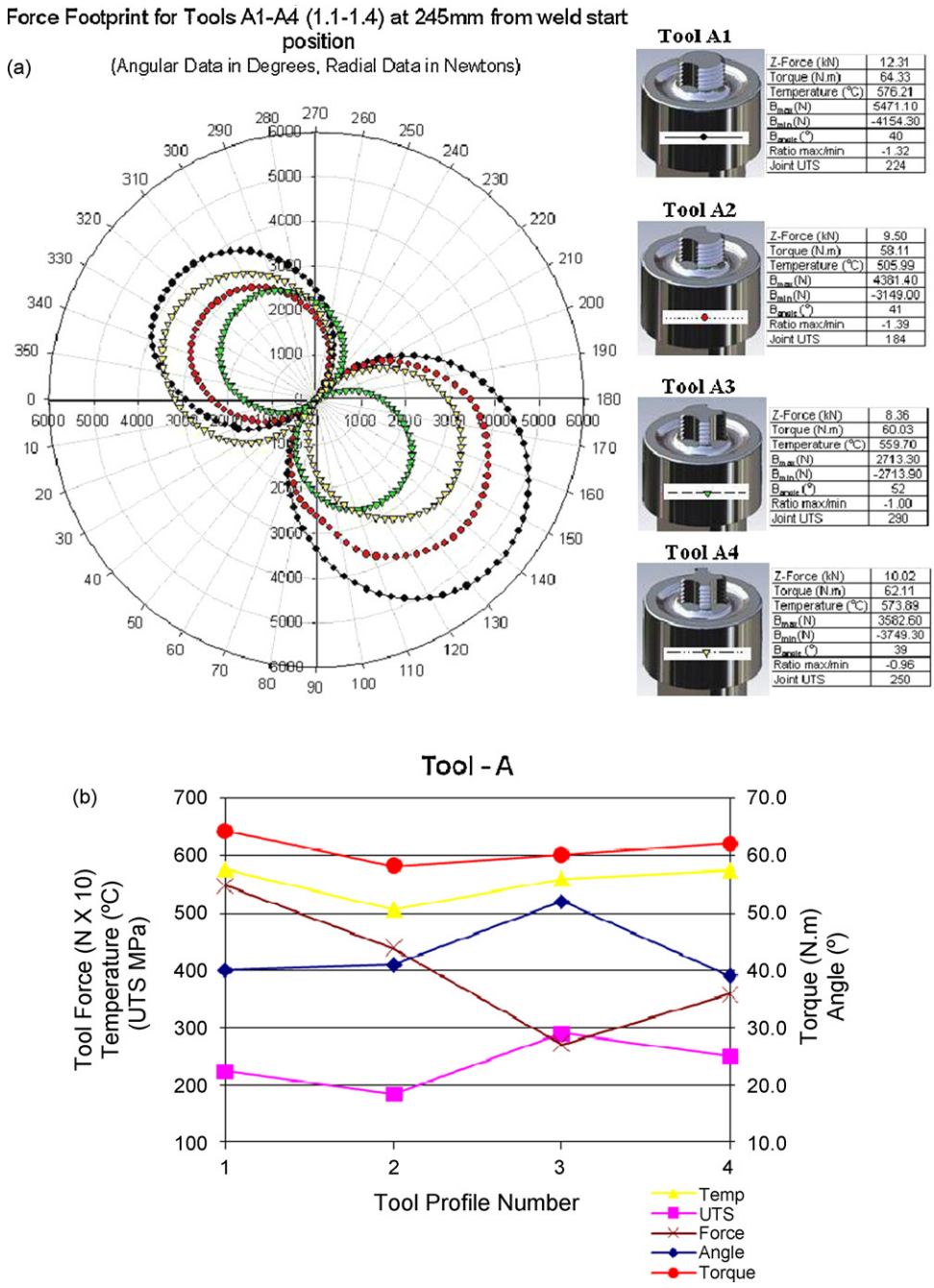

Fig. 3 – (a) FF diagrams and corresponding process data for the A-series tools and (b) process data for A-series tools where there is an increase in number of flutes from A1 to A4.

graphically presents the information on variation of process parameters contained in the tables. The only relevant parameter not included in Fig. 3b is the value of the downwards (z-direction) forging force during welding. It is clear that the required output property of tensile strength passes through a local maximum in this tool set. Correlations apparently exist in this case between certain of the measured parameters and the tensile strength. Thus weld tensile strength and angular rotation of the position of the maximum lateral force on the tool display similar trends, while the value of the maximum lateral force has an inverse correlation with tensile strength. The maximum value of tensile strength over the range of tool profiles corresponds with a minimum in lateral maximum force and a maximum rotation of the position of this maximum force; in other words with favourable plastic flow conditions in the TMAZ. Tool temperature and torque follow related trends and this is generally true for all tool sets with specific exceptions in the F- and P-series tools.

These results can be interpreted in the following way. A substantial amount of the heat input into the weld is generated under the tool shoulder, but the pin has a strong

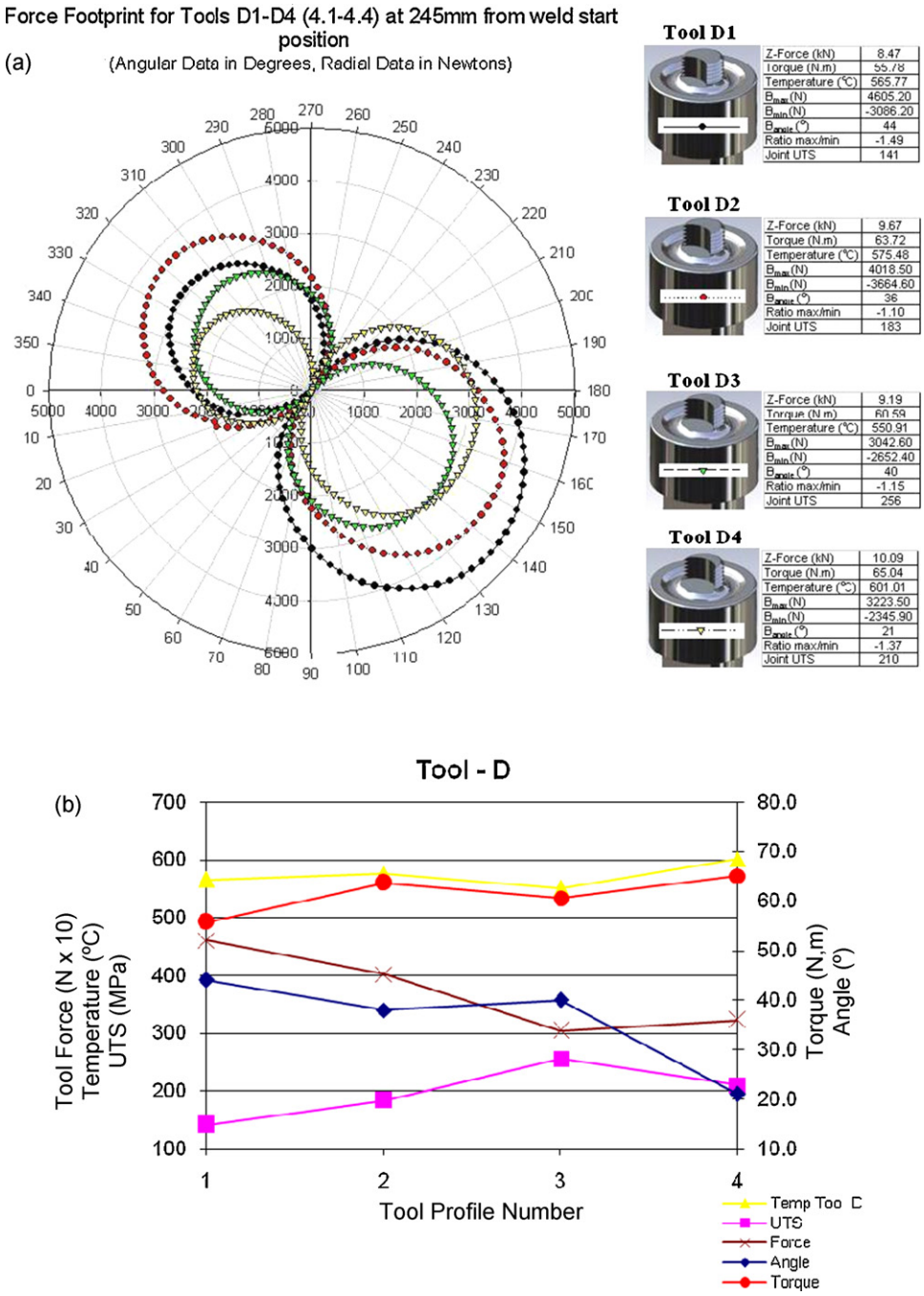

Fig. 4 – (a) FF diagrams and corresponding process data for the D-series tools and (b) process data for D-series tools where there is an increase in flute depth from D1 to D4.

influence on plastic flow and hence on tensile strength. Torque is strongly related to tool temperature but is also influenced by specific geometric details of the tool pin. Thus pin diameter (P-series tools) and conical flute angle (F-series tools) both have strong influences on plasticity and on welding torque, such that specific geometries give significant torque reductions (~20–30%) without associated reductions in tool temperature. The low torque geometries in the P- and F-series tools correlate with high tensile strengths and hence indicate favourable plastic flow and mixing conditions in the thermo-mechanically affected zone of the weld.

It would be expected that an optimum number of flutes would exist in terms of effective plastic flow around the pin and thus joint strength, and this is supported by the experimental results. Thus the 3-flute tool gave the highest weld tensile strength, the largest rotational angle for maximum lateral force and the minimum value of maximum lateral force found with the four tools (around 50% of the force measured with the single flute pin. Torque, temperature and tensile strength all show minima with the 2-flute tool, implying that the plasticised zone is rotating with the tool, rather than undergoing proper mixing of the entrained alloy. The

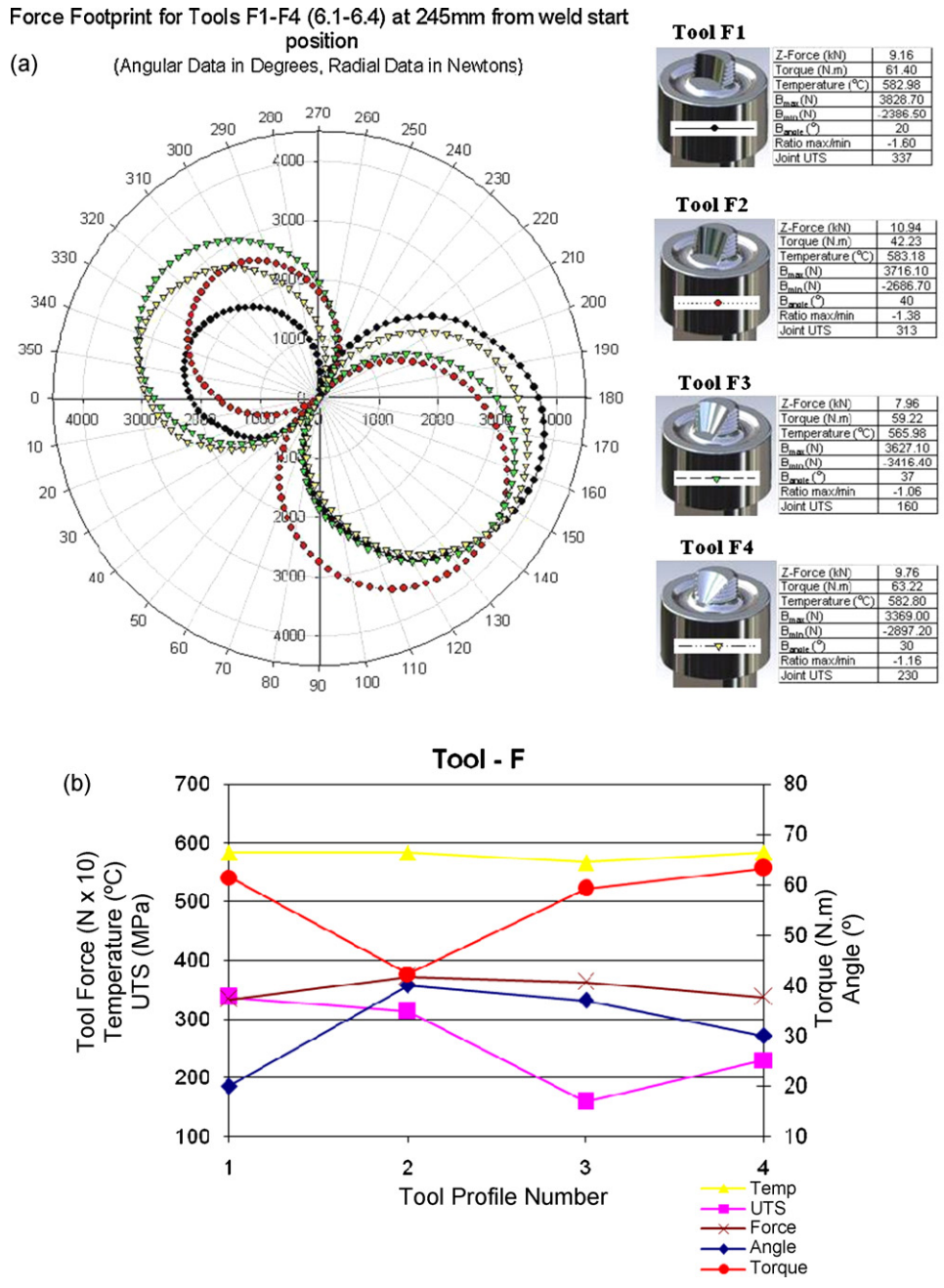

Fig. 5 – (a) FF diagrams and corresponding process data for the F-series tools and (b) process data for F-series tools where there is an increase in flute angle from F1 to F4.

3-flute tool also gives the lowest value of z-force; a reduction of some 32% over the single flute tool (from 12.31 to 8.36 kN).

5. Flute depth (D-series tools)

These tools are machined with a progressive 1 mm increase in depth of the single flute going from tool D1 to D4. The cutter diameter was 10 mm and the resultant flute profiles are shown in Fig. 2b. Fig. 4a and b shows analogous data to that shown in Fig. 3 for the A-series tools. This format will be followed for all the tools discussed in this paper. The maximum value of weld tensile strength in this series occurs with tool D3 which also exhibits the minimum value of the maximum lateral force, as was found with the A-series tools. In this case, however, the angular rotation of the maximum lateral force on the tool does not display such a close correlation with the trend in tensile strength in going from D1 to D4, possibly reflecting the increasing bulk entrainment of metal attendant on the larger flute scallop. Torque and temperature follow very similar trends in these D-series tools to those found with the A-series tools (see Table 3), but with generally higher tool tempera-

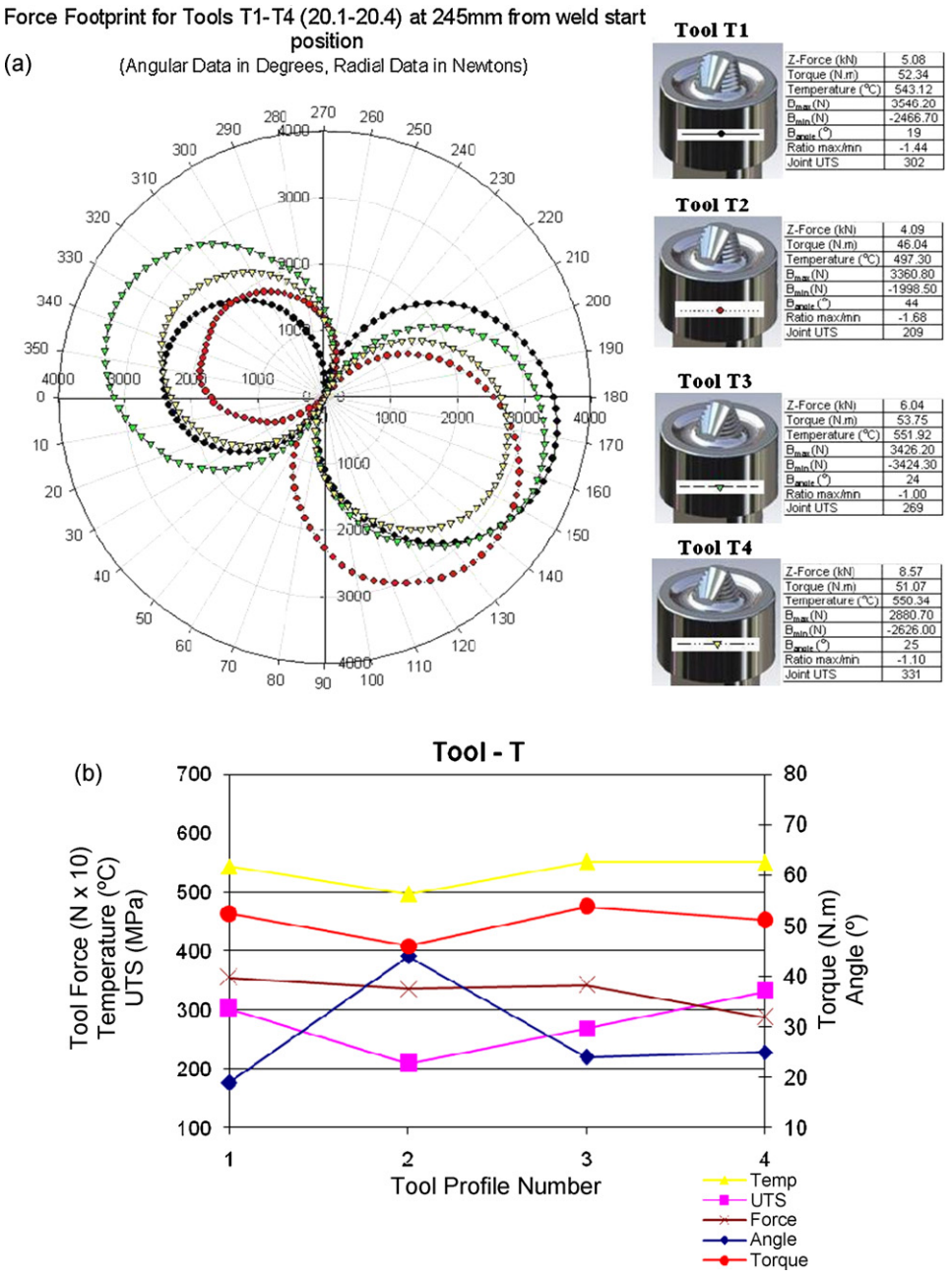

Fig. 6 – (a) FF diagrams and corresponding process data for the T-series tools and (b) process data for T-series tools where there is an increase in pin taper angle from T1 to T4.

tures (551–601 °C) and a wider range of tool torque values (55.8–65.0 Nm).

The maximum value of tensile strength in this series occurs with tool D3 and is some 12% lower at 256 MPa (74% of the parent plate value) than found with the A-series tools (290 MPa = 83% of the parent plate value). It is immediately clear that increasing the number of flutes is a better tool optimisation strategy than increasing the depth of a single flute. The issue of determining the optimum depth of flute on a multi-flute tool remains to be addressed in future work.

6. Flute angle (F-series tools)

In F-series tools the angle of the conical taper was increased, as shown in Fig. 2c, by keeping the depth of the flute constant at the end of the pin and progressively decreasing the subtended angle of the flute at the pin-shoulder intersection. Fig. 5a and b presents the data summary for this tool series. As might be expected, the effectiveness of this tool series in making high strength joints decreases steadily from F1 to F3 but, interestingly, increases again for tool F4. The

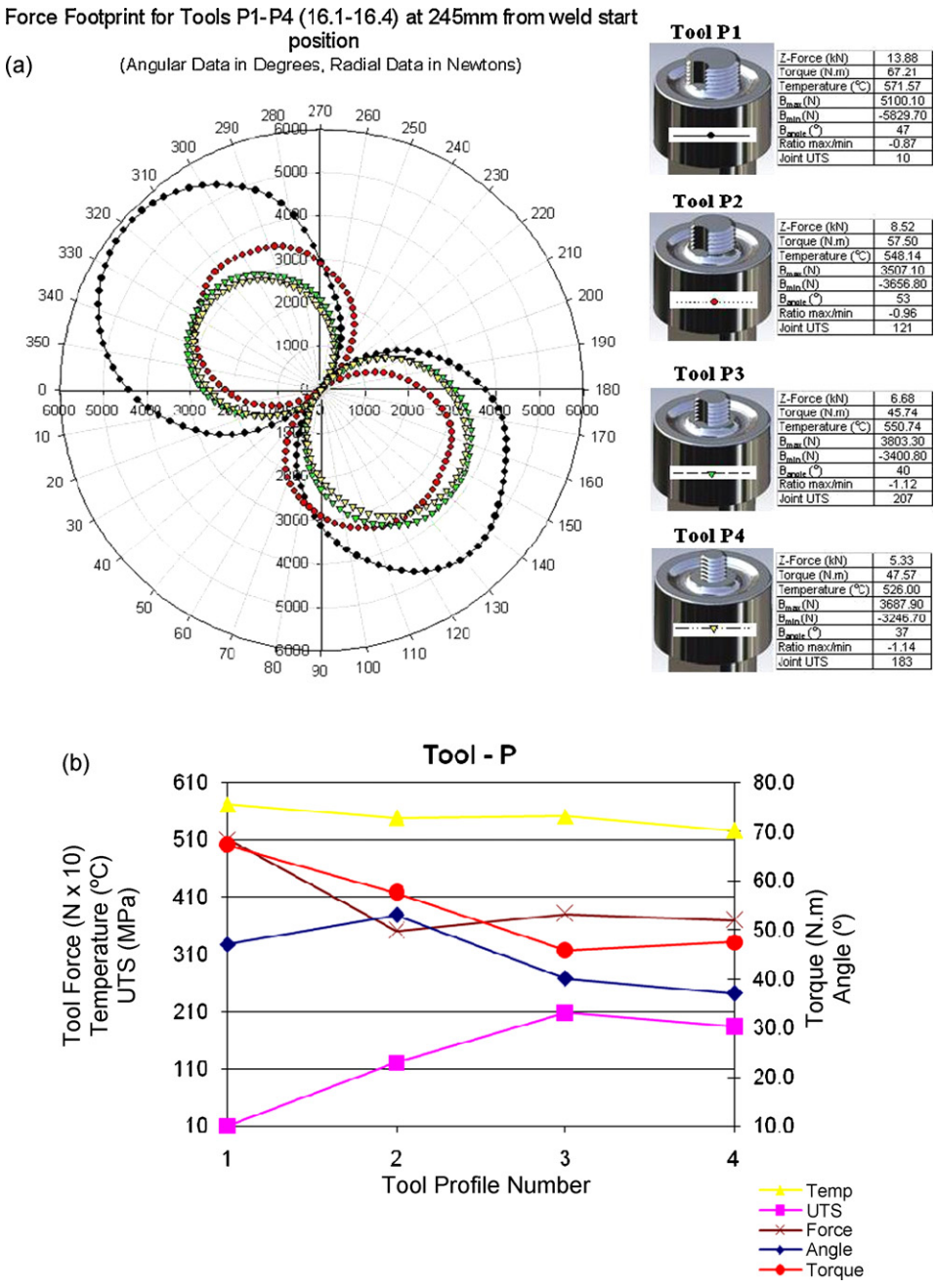

Fig. 7 – (a) FF diagrams and corresponding process data for the P-series tools and (b) process data for P-series tools where there is an increase in pin diameter from P1 to P4.

only relatively clear correlation between weld process parameters for these tools is the inverse relationship between torque and angular rotation of the maximum value of lateral force on the tool. Tool F1 is similar to tool D3 but gives a tensile strength value of 337 MPa, some 32% higher than tool D3. The implication of this result is that a flute taper is beneficial in producing the plastic flow conditions that lead to high strength welds for similar tool geometries. This is perhaps not surprising, as it might be expected that a tapered shape would aid void-free mixing of entrained streams of metal. The highest value of tensile strength corresponds with a low value of angular rotation of the maximum force (20°). F-series tools produced welds with the highest and third highest values of tensile strength found in this investigation (F1 = 337 MPa or 97% of the parent plate value; F2 = 313 MPa, or 90% of the parent plate value). Welds F1 and F2 did not show discernible evidence of voids in tensile specimens or in metallographic samples.

The range of tensile strengths (160–337 MPa) with F-series tools is larger than found with the A-series tools (184–290 MPa) or the D-series tools (141–256 MPa) and has a higher peak value. Optimising the angle of a single flute appears to offer more potential for weld strength improvement in this alloy than increasing the number of flutes.

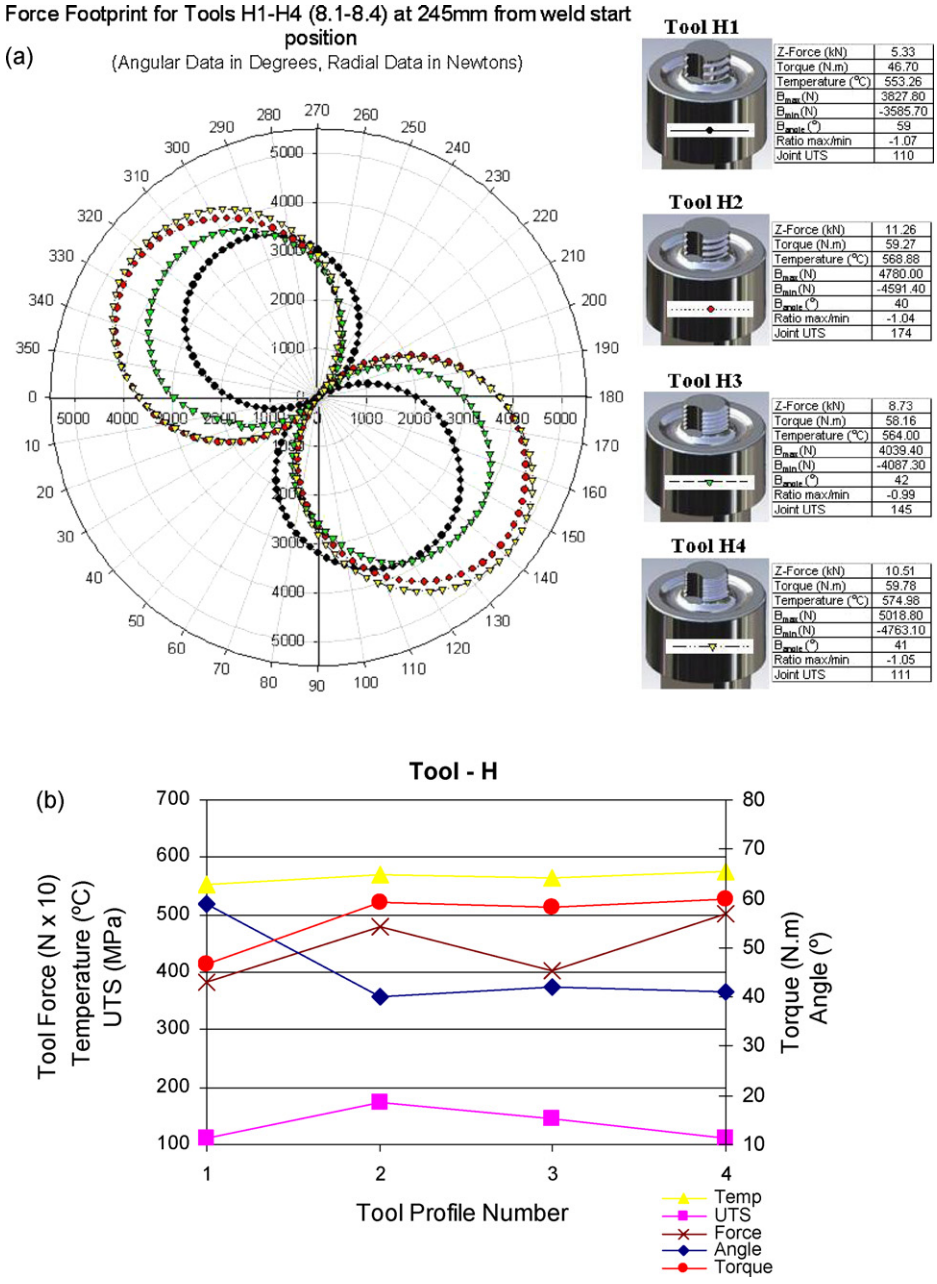

Fig. 8 – (a) FF diagrams and corresponding process data for the H-series tools and (b) process data for H-series tools where there is an increase in thread pitch from H1 to H4.

7. Pin taper angle (T-series tools)

Essentially this tool series can be viewed as a development on the F3 tool, where tool taper is progressively added to a tapered scallop. The tools are tapered from a diameter of 10 mm at the shoulder to give taper ratios from 1.25 for tool T1 (8 mm diameter at the free end) to 2 for tool T4 (5 mm at the free end). The T-series tools are shown in Figs. 2d and 6a. The data for this tool series is summarised in Fig. 6a and b. This tool series produced welds with consistently high values of tensile strength and it is clear that the highest strengths correspond with low values of angular rotation of the maximum force (around 19–25°). T-series tools produced welds with the second and fourth highest values of tensile strength found in this investigation (T4 = 331 MPa, or 95% of the parent plate value; T1 = 302 MPa, or 87% of the parent plate value). Tool T4 also produced defect-free welds, while T1 did not.

Maximum values of bending force during welding decreased steadily as the taper ratio increased from 1.25 to 2, showing a decrease of 19% from tool T1 to T4. On the basis of these results, and these pin-to-shoulder diameter ratios, adding a pin taper to FSW tools is a useful route to weld process optimisation and, as suggested for the F-series tools, it seems that a taper is beneficial in producing the plastic flow conditions that are conducive to high strength welds.

Table 4 – Angular force rotation and tensile data for the best performing tool in each series

Tool type	Tensile strength (MPa)	Ratio of weld to PP strength (%)	Angular rotation of peak Force (°)	Ratio of max/min force
F1	337	97	20	−1.60
T4	331	95	25	−1.10
A3	290	83	52	−1.00
D3	256	74	40	−1.15
P3	207	59	40	−1.12
H2	174	50	40	−1.04

8. Pin diameter (P-series tools)

P-series were characterised by a change in pin diameter from 12 to 6 mm in steps of 2 mm, respectively, as shown in Figs. 2e and 7a. Fig. 7a and b presents force footprint and process parameter data for these tools. Tool P1 produced welds with the lowest tensile strength found in this experimental matrix; a very low value of 10 MPa which reflects the very severe wormhole voiding found with this tool. The range of lateral bending force on the tool was the highest recorded in the experimental matrix which indicates that little effective plasticized stirring of the alloy is occurring. Torque values are very high for tool P1 and progressively decrease across tools P2 and P3 before increasing slightly with tool P4. Temperature and force are also highest with tool P1. The tool is effectively 'ploughing' through the material rather than stirring and recombining plasticized material to form a weld. The force footprint also indicates that, uniquely, for this tool the peak force value on the advancing side of the tool is higher than the peak force on the retreating side. This therefore appears to be an indicator of severe void formation during welding. The highest tensile strength in this series is produced by tool P3 (some 59% of the parent plate value).

9. Thread pitch (H-series tools)

Figs. 2f and 8a show details of the H-series tools which explore the effect of thread pitch on weld process parameters and tensile strength. Tools in this series are essentially variants of tool A1 (with a 1 mm pitch) with pitches ranging from 1.57 mm (16 threads per inch) to 0.9 mm (28 threads per inch). The thread on each pin was machined opposite to that of the spindle rotational direction to assist with plastic flow and to provide a downwards auguring effect. The lowest values of tensile strength in this series were found with tools H1 and H4. The highest tensile strength occurred with tool H2; some 174 MPa or 50% of the parent plate value. Clearly the chosen pitch value of 1mm across all tool series is a good compromise for this set of welding conditions. This is 10% of the pin diameter and 17% of the plate thickness.

10. Conclusions

This paper is one of the first studies that has systematically examined and reported influences of tool geometry factors on friction stir welding process parameters and on weld tensile strength. Several points can be drawn out from the discussion of the results above to provide some general guidelines on tool design. The data in this study have been obtained for a specific alloy AA5083-H321 and plate thickness (6 mm), but it is known that certain of the tool parameters have been identified as important in welding other alloys and plate sizes, e.g. the 3-flute concept is proven in thread taps and widely used in the tri-flute tools developed at TWI. Thus these guidelines may be applicable to a range of alloys and plate thicknesses. The guidelines are unlikely to be definitive as other tool parameters not considered in this study may be influential on forces, torque, plastic stirring and hence tensile strength. It is also worth noting that the extensive internal voiding observed with certain tools implies that the forging role of the tool shoulder may be rather limited and that a rotating shoulder may be an inefficient part of the welding process.

Table 4 presents the angular rotation of the maximum bending force on the tool, the ratio of maximum to minimum force and the weld tensile data for the best performing tool in each series. The data support the hypothesis that the force footprint diagram contains information relevant to interpreting the success of plastic flow and stirring in the weld TMAZ. The highest strength welds correspond with low angular rotation values of the maximum force and high ratios of maximum to minimum force on the tool. Optimised tool design can produce welds with 97% of the parent plate tensile strength in this strain hardening 5083-H321 aluminium alloy.

The data indicate that the most successful tool designs are likely to incorporate three tapered flutes, a pin diameter taper and have a thread form with a pitch of around 10% of the pin diameter and perhaps 15% of the plate thickness. Further work is required to determine the generality of these conclusions.

Acknowledgments

Thanks are due to Dr. Grant Kruger at NMMU who provided assistance with the development of the monitoring and data logging system, and to the National Research Foundation (NRF), South Africa for financial support.

REFERENCES

Arbegast, W.J., 2005. Using process forces as a statistical process control tool for friction stir welds. In: Proceedings of the Friction Stir Welding and Processing III, 2005 TMS Annual Meeting, San Francisco, CA, USA, February 13–17, pp. 193–204.

Blignault, C., 2003. Design, Development and Analysis of the Friction Stir Welding Process. MTech Thesis, Port Elizabeth Technikon, South Africa.
Blignault, C., 2006. A Friction Stir Weld Tool-force and Response Surface Model Characterizing Tool Performance and Weld Joint Integrity. DTech Thesis, Nelson Mandela Metropolitan University, South Africa.
Blignault, C., Hattingh, D.G., Kruger, G.H., van Niekerk, T.I., James, M.N., 2008. Friction Stir Weld Process Evaluation by Multi-Axial Transducer. Measurement 41, 32–43.
Hattingh, D.G., van Niekerk, T.I., Blignault, C., Kruger, G., James, M.N., 2004. Analysis of the FSW force footprint and its relationship with process parameters to optimise weld performance and tool design, Invited Paper (INVITED-2004-01), IIW Journal Welding in the World, vol. 48. No. 1–2, pp. 50–58.
James, M.N., Bradley, G.R., Lombard, H., Hattingh, D.G., 2005. The relationship between process mechanisms and crack paths in friction stir welded 5083-H321 and 5383-H321 aluminium alloys. Fatigue Fract. Eng. Mater. Struct. 28, 245–256.
Lombard, H., 2007. Optimised Fatigue and Fracture Performance of Friction Stir Welded Aluminium Alloy Plate: A Study of the Inter-relationship Between Process Parameters, TMAZ, Microstructure, Defect Population and Performance. PhD Thesis, University of Plymouth, England.
Lombard, H., Hattingh, D.G., Steuwer, A., James, M.N., 2008. Optimising FSW process parameters to minimise defects and maximise fatigue life in 5083-H321 aluminium alloy. Eng. Fract. Mech. 75, 341–354.
Schmidt, H., Hattel, J., 2005. An analytical model for prescribing the flow around the tool probe in friction stir welding. In: Proceedings of the Friction Stir Welding and Processing III, 2005 TMS Annual Meeting, San Francisco, CA, USA, February 13–17, pp. 193–204.